J Neurophysiol 109: 557–569, 2013.
First published October 24, 2012; doi:10.1152/jn.00549.2012.

On the origin of event-related potentials indexing covert attentional selection during visual search: timing of selection by macaque frontal eye field and event-related potentials during pop-out search

Braden A. Purcell, Jeffrey D. Schall, and Geoffrey F. Woodman
Department of Psychology, Center for Integrative & Cognitive Neuroscience, Vanderbilt Vision Research Center, Vanderbilt University, Nashville, Tennessee

Submitted 22 June 2012; accepted in final form 23 October 2012

Purcell BA, Schall JD, Woodman GF. On the origin of event-related potentials indexing covert attentional selection during visual search: timing of selection by macaque frontal eye field and event-related potentials during pop-out search. *J Neurophysiol* 109: 557–569, 2013. First published October 24, 2012; doi:10.1152/jn.00549.2012.—Event-related potentials (ERPs) have provided crucial data concerning the time course of psychological processes, but the neural mechanisms producing ERP components remain poorly understood. This study continues a program of research in which we investigated the neural basis of attention-related ERP components by simultaneously recording intracranially and extracranially from macaque monkeys. Here, we compare the timing of attentional selection by the macaque homologue of the human N2pc component (m-N2pc) with the timing of selection in the frontal eye field (FEF), an attentional-control structure believed to influence posterior visual areas thought to generate the N2pc. We recorded FEF single-unit spiking and local field potentials (LFPs) simultaneously with the m-N2pc in monkeys performing an efficient pop-out search task. We assessed how the timing of attentional selection depends on task demands by direct comparison with a previous study of inefficient search in the same monkeys (e.g., finding a T among Ls). Target selection by FEF spikes, LFPs, and the m-N2pc was earlier during efficient pop-out search rather than during inefficient search. The timing and magnitude of selection in all three signals varied with set size during inefficient but not efficient search. During pop-out search, attentional selection was evident in FEF spiking and LFP before the m-N2pc, following the same sequence observed during inefficient search. These observations are consistent with the hypothesis that feedback from FEF modulates neural activity in posterior regions that appear to generate the m-N2pc even when competition for attention among items in a visual scene is minimal.

electroencephalogram; covert selection; visual salience; visual attention; top-down control

EVENT-RELATED POTENTIALS (ERPs) provide crucial information on the timing of specific cognitive operations (Luck 2005). Attention-related ERPs can track shifts in attentional allocation in humans processing complex scenes (Woodman and Luck 1999, 2003). Specifically, the N2pc component provides an index of attentional allocation across the visual field (Luck and Hillyard 1994a, b), but a thorough investigation into the neural mechanisms that generate the N2pc is precluded by the difficulty in obtaining intracranial recordings from human subjects. Current source density and source estimation procedures suggest that the N2pc is generated by attentional modulations in posterior visual regions (Boehler et al. 2011; Hopf et al. 2000, 2004; Luck and Hillyard 1994a), but these methods are under constrained without intracranial data (Helmholtz 1853; Luck 2005; Nunez and Srinivasan 2006) and cannot resolve hypotheses concerning the influence of more distal regions that drive the underlying neural generator.

We have addressed this methodological shortcoming by simultaneously recording ERPs with intracranial signals in nonhuman primates (Woodman 2011). We recently identified a macaque homologue of the N2pc component, termed the m-N2pc, which is a relative positivity contralateral to an attended item (Cohen et al. 2009a; Heitz et al. 2010; Woodman et al. 2007). The human N2pc was originally hypothesized to be due to feedback from attentional control structures because of its relatively long latency and sensitivity to task demands (Luck and Hillyard 1994a), but until recently, it has been impossible to test this hypothesis directly. ERPs lack the spatial resolution to distinguish the attention-related modulations in visual cortex from control structures in frontal cortex thought to drive those modulations. This has led to controversy about the degree to which the N2pc reflects bottom-up vs. top-down attentional signals (Eimer and Kiss 2010; Theeuwes 2010). With the establishment of a homologous component in monkeys, we can test this hypothesis using targeted, invasive procedures that are impossible in healthy humans.

The frontal eye field (FEF) is a region of prefrontal cortex thought to be involved in attentional control. FEF single-unit spiking and local field potentials (LFPs) evolve to identify the location of behaviorally relevant search targets (Bichot and Schall 1999; Cohen et al. 2009a, b; Monosov et al. 2008; Sato et al. 2001; Thompson and Bichot 2005), whether or not a saccade is generated (Thompson et al. 1997, 2005). For this reason, FEF has been identified with a salience map that guides attentional deployment (Thompson and Bichot 2005), possibly via projections to extrastriate visual cortex (Anderson et al. 2011; Ninomiya et al. 2011; Pouget et al. 2009). The role of FEF in top-down attentional control is further supported by the effects of FEF microstimulation on activity in extrastriate visual cortex (Ekstrom et al. 2008; Moore and Armstrong 2003). Thus FEF is a prime candidate for an attentional-control structure that could drive the neural generator of the N2pc.

We recently found that FEF neurons and LFPs select the location of search targets before the m-N2pc during an inefficient visual search task (Cohen et al. 2009a). This result is consistent with the hypothesis that feedback from FEF participates in driving the putative posterior generator of the m-N2pc. This hypothesis is also supported by intracranial

Address for reprint requests and other correspondence: G. F. Woodman, Dept. of Psychology, Vanderbilt Univ., PMB 407817, 2301 Vanderbilt Pl., Nashville, TN 37240-7817 (e-mail: geoffrey.f.woodman@vanderbilt.edu).

recordings demonstrating that attentional selection occurs in the prefrontal cortex before lateral intraparietal area (LIP) (Buschman and Miller 2007), visual cortex area V4 (Zhou and Desimone 2011), and inferior temporal (IT) (Monosov et al. 2010) during attentionally demanding tasks. However, it is not clear how this timing depends on task demands. For example, one study has found that the ordering of selection across cortex depends on search difficulty (Buschman and Miller 2007), which could influence the timing of the N2pc relative to FEF. In addition, a recent study reported an N2pc in response to a task-irrelevant singleton (Hickey et al. 2006), suggesting that this component may not depend on top-down influences. Moreover, some theories of visual attention propose that an efficient search for a target defined by a single feature can be performed pre-attentively (Treisman and Gelade 1980). Thus it could be the case that the onset of the N2pc followed attentional selection in FEF because the task required explicit top-down control, but the same may not hold true during efficient search tasks.

To determine the degree to which the timing of selection in FEF and the m-N2pc depends on attentional demands, we recorded ERPs from monkeys performing an efficient pop-out visual-search task simultaneously with FEF single-unit activity and LFPs. The experimental protocol, analytical and statistical methods, and monkeys were the same as those used in a previous report on attentional selection during inefficient T vs. L search to allow for direct comparison across studies (Cohen et al. 2009a). If these three signals reflect the timing of attentional allocation, then the timing of selection should modulate with set size when search is inefficient but not when search is efficient. In addition, if efficient search requires feedback from the saliency map of FEF to the neural generator of the m-N2pc, then we would expect selection in FEF to precede or coincide with the m-N2pc, as was observed during inefficient search. We would also expect to see trial-by-trial correlations between FEF activity and the m-N2pc.

MATERIALS AND METHODS

Behavioral Tasks and Recordings

Recording procedure. We simultaneously recorded neuronal spikes, LFPs, and the extracranial EEG from two male macaques (*Macaca radiata*; identified as Q and S). Monkeys were surgically implanted with a head post, a subconjunctive eye coil, and recording chambers during aseptic surgery under isoflurane anesthesia. Antibiotics and analgesics were administered postoperatively. All surgical and experimental procedures were in accordance with the National Institute of Health Guide for the Care and Use of Laboratory Animals and were approved by the Vanderbilt Institutional Animal Care and Use Committee.

Neurons and LFPs were recorded from the right and left FEF of both monkeys using tungsten microelectrodes (2–4 MΩ; FHC, Bowdoin, ME) and were referenced to a guide tube in contact with the dura. All FEF recordings were acquired from the rostral bank of the arcuate sulcus at sites where saccades were evoked with low-intensity electrical microstimulation (<50 μA) (Bruce et al. 1985). Spikes were sampled at 40 kHz, and LFPs were sampled at 1 kHz. LFPs were band-pass filtered between 0.2 and 300 Hz and amplified using an HST/8o50-G1 headstage (Plexon, Dallas, TX). LFPs were baseline corrected using the average voltage during the window from 100 to 0 ms before array presentation. Spikes were sorted online using a time-amplitude window discriminator and offline using principal component analysis and template matching (Plexon). We generated spike-density functions by convolving each spike train with a kernel resembling a postsynaptic potential (Thompson et al. 1996).

Following the method of Woodman et al. (2007), we recorded ERPs from gold skull electrodes implanted 1 mm into the skull. Electrodes were located at approximately T5/T6 in the human 10–20 system scaled to the macaque skull. EEG signals were sampled at 1 kHz and filtered between 0.2 and 300 Hz. A frontal EEG electrode (approximating human Fz) was used as the reference for the lateral, posterior EEG signals.

Behavioral tasks. The monkeys performed a pop-out visual search task and a memory-guided saccade task; the latter allowed for the classification of different cell types. All tasks began with the monkey fixating a central white spot for ~500 ms. In the pop-out visual search task (see Fig. 1*A*), the fixation point changed from a filled to an unfilled white square (10.3 cd/m^2) simultaneously with the presentation of a colored target and one, three, or seven distractors of the opposite color. The number of distractors varied randomly across trials. Targets and distractors were either red [Commission Internationale de l'éclairage (CIE) chromaticity coordinates, $x = 0.620$; $y = 0.337$] or green (CIE, $x = 0.289$; $y = 0.605$). The target and distractor color remained constant throughout the session, and target color was varied across sessions. The monkey was rewarded for making a single

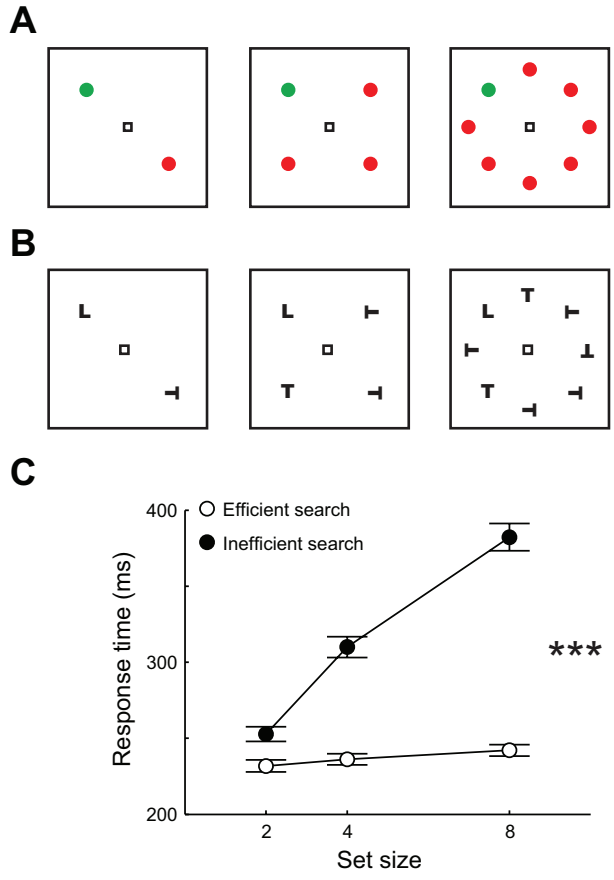

Fig. 1. Visual search task and behavior. *A*: after fixating for a variable delay, a search array appeared consisting of 1 target (e.g., green disk) and 1, 3, or 7 distractors (e.g., red disks). Monkeys were required to make a single saccade to the target for a reward. Target identity varied across sessions. *B*: we directly compared our new results from efficient pop-out search with previously published data collected from the same monkeys performing an inefficient visual search task (Cohen et al. 2009a). All procedures were identical to efficient search except that the monkeys searched for a T among Ls (or vice versa). *C*: mean response time (RT) to the target as a function of set size for both search tasks. Error bars represent SE around the mean of the session means. ***$P < 0.001$, significant differences in slope across tasks.

saccade to the location of the target within 2,000 ms of array presentation and fixating that target for 500 ms.

Each neuron was also recorded during a memory-guided saccade task to distinguish visual- from movement-related activity (Bruce and Goldberg 1985; Hikosaka and Wurtz 1983). In this task, a target (filled gray disk) was presented for 100 ms at one of eight isoeccentric locations, equally spaced around the fixation spot at 10° eccentricity. The animal was required to maintain fixation for 400–800 ms (uniform distribution) after the target presentation. After the fixation point changed from a filled square to an unfilled square, the monkeys were rewarded for making a saccade to the remembered location of the target and maintaining fixation at that remembered location for 500 ms.

We also analyzed previously published FEF neurons, FEF LFPs, and the m-N2pc recorded from the same monkeys during an inefficient visual search (Fig. 1*B*) (Cohen et al. 2009a, b; Woodman et al. 2008). The task was identical to the pop-out search task described above, except that monkeys searched for a target defined by form [T or L in one of four orientations; see details regarding the metrics of the stimuli in Cohen et al. (2009a)] among distractors (Ls or Ts, respectively). Target identity varied across sessions. Analytical and procedural methods were identical for data collected during both tasks. This allowed us to perform statistical comparisons between our new data collected during pop-out search and previously published data collected during inefficient search.

Data Analysis

Neuron classification. We identified task-related neurons and LFPs by comparing activity with the baseline period, 50 ms before presentation of the array. A neuron or LFP signal was classified as visually responsive if activity (discharge rate or voltage) was significantly different from baseline in the interval 50–200 ms following stimulus presentation during the memory-guided saccade task and in the interval 50–150 ms during search ($P < 0.05$, Wilcoxon rank sum test). A neuron or LFP was classified as saccade related if activity was significantly different from baseline in the interval −100 to 100 ms relative to saccade initiation for all tasks. Unless otherwise noted, our analyses focused on visually responsive units with or without saccade-related modulation, because these are the neurons known to represent visual salience (Bichot and Schall 1999; Sato et al. 2001; Thompson and Bichot 2005) and are likely to project to posterior visual areas thought to generate the N2pc (Gregoriou et al. 2012; Pouget et al. 2009; Thompson et al. 1996). Of the 102 total neurons that we recorded, 84 neurons (82%) exhibited significant visual responses. Of the 141 total LFP sites that we recorded, 133 LFPs (94%) exhibited significant visual responses. Of the 84 sites, in which visually responsive neurons were recorded, 81 (96%) also exhibited visually responsive LFPs. Thus the sample size was 81 for the paired comparisons of simultaneously recorded neurons, LFPs, and ERPs. Of the 99 visually responsive LFP sites, in which neurons were concurrently recorded, 18 neurons (18%) did not exhibit visual responses.

Selection time. We used a "neuron-antineuron" approach to determine the selection time when the target location could be discriminated reliably in single-unit spiking, LFPs, and ERPs (Britten et al. 1992; Thompson et al. 1996). The onset of the m-N2pc component is identified as the time when ERPs recorded at posterior-lateralized electrodes become different based on the location of the attended target item (i.e., selection time). Here, the selection time is defined as the time at which the distribution of activity—when the search target is inside of a receptive field (RF)—is significantly greater than the distribution of activity when the target is opposite of the RF for 10 consecutive ms with a conservative α value of 0.01 (Wilcoxon rank sum test). These criteria are identical to a previous report (Cohen et al. 2009a). For all signals, we defined the RF (or preferred location) as the three adjacent target locations in which the firing rate or voltage modulation maximally deviated from baseline. To ensure that our results were not the artifact of the orientation of the corneoretinal potential that changed during the saccade (Godlove et al. 2011b), we also computed selection time with signals aligned on saccade initiation. Only signals that selected the target >20 ms before saccade initiation were included in this analysis.

For direct comparison with a previous study, we also estimated selection time by running an ANOVA at each millisecond following target presentation (Monosov et al. 2008). The resulting *P* value gave the probability that the activity did not vary across target locations. The selection time was the first millisecond that the *P* value dropped below 0.05 before continuing past 0.001 and remaining below 0.05 for 20 out of 25 subsequent ms. This ensured that differences across studies cannot be explained by differences in analytical methods. This method also ensures that our results are not due to our definition of RFs.

We also computed population selection times based on all 102 FEF single units, 141 LFPs, and the m-N2pc, conditionalized on whether the target was contralateral or ipsilateral to the hemisphere over which the signal was recorded. This approach is more similar to human electrophysiological studies in which the N2pc is identified by averaging the waveforms from the posterior-lateralized electrodes based on whether attention is allocated to the contralateral or ipsilateral visual field. This included neurons and LFP with and without significant visual responses and with both contralateral and ipsilateral preferred locations. Since the average firing rates of cortical neurons vary markedly, we normalized responses between 0 and 1 by subtracting the minimum response and dividing by the range so that variability across recording sites did not inflate selection times. The population selection time is defined as the time when the distributions of activity—when the target is contralateral and ipsilateral—significantly diverge for 10 consecutive ms, with $\alpha = 0.01$ (Wilcoxon rank sum test). Here, the distribution is across neurons and recording sites, whereas individual selection times were based on the distribution across trials. All signals were truncated at saccade.

Magnitude of selection. We quantified the magnitude of selection as the difference in response magnitude when the target or a distractor was in the RF (preferred location) for each signal. For spiking activity, the magnitude of selection was computed as the difference in average normalized firing rate from 125 to 200 ms after the array presentation. For LFPs and the m-N2pc, the magnitude of selection was computed as the integral of the voltage in the same time window divided by the length of the window (Cohen et al. 2009a). All signals were truncated at saccade.

Set size effects. To assess how response time (RT), selection time, and magnitude of selection depended on set size and search efficiency, we fit a multiple linear regression model of the form: $y = \beta_0 + \beta_1 s + \beta_2 e$, where the independent variable, *y*, is the mean RT for each session, the selection time, or the magnitude of selection for each single unit, LFP, or ERP. The predictor *s* is the set size (in items), and the predictor *e* is a dummy variable representing search efficiency (0 = efficient; 1 = inefficient). We assessed whether the coefficient β_1 was significantly different from zero to test for significant set size effects. We assessed whether the coefficient β_2 was significantly different from zero to test for a significant effect of search efficiency.

Visual response latency. The latency of the visual response was determined by comparing baseline activity with activity during a millisecond-by-millisecond sliding window, starting at array presentation. For FEF spiking activity and LFPs, the visual onset was the time when activity first became significantly different from baseline and remained significant for 10 consecutive ms ($P < 0.01$, Wilcoxon rank sum test). For ERPs, we required significance to be maintained for 30 consecutive ms to eliminate false alarms indicated by bimodality in the distribution and visual inspection.

Trial-by-trial correlations of spike rate, LFP, and ERP amplitude. We computed the Pearson correlation coefficient between the trial-by-trial amplitude modulation of simultaneously recorded neurons, LFPs, and ERPs. We used only signals that selected the target in these analyses. For spiking activity, amplitude was computed as the average firing rate in the window from 150 ms after the array presentation until

the saccadic response to exclude the nonselective initial visual response. For LFPs, amplitude was computed as the integral of the voltage in the same time window divided by the length of the window. We compared simultaneously recorded neurons and LFPs that were recorded from the same electrode or spaced ~1 mm apart. For comparison with a previous study (Cohen et al. 2009a), the ERP amplitude was first computed as the integral of the voltage in the same time window divided by the length of the time window. However, it is possible for this method to yield spurious correlations due to common noise picked up at the frontal reference. As a control, we also computed the ERP amplitude as the integral of the voltage difference between the two posterior electrodes divided by the length of the time window. We computed the correlation using trials in which the target appeared inside of the RF of the neuron and LFP. As an additional control, we computed the correlation during the baseline period, 100 ms before array presentation. This allowed us to determine the inherent correlations between these signals, independent of those elicited by the analysis of the elements in the search arrays. For this analysis, we baseline corrected 250–150 ms before the time window (i.e., 350–250 ms before array presentation).

Control for differences in signal-to-noise ratio. We measured the change in selection time with the number of trials to test whether differences in the signal and noise characteristics of the neural measures could explain observed differences in selection time. Following the methodology of Cohen et al. (2009a), we characterized the change in selection time as a function of trial number (randomly sampled, with replacement) using an exponential function of the form: $ST = ST_{max + min}\, e^{-n/\tau} + ST_{min}$, where ST is selection time; n is the number of trials; τ is the decay (in units of trials); $ST_{max + min}$ is the baseline (ms); and ST_{min} (ms) is the asymptote. We optimized parameters to fit selection time as a function of the number of trials individually for each neuron, LFP site, and ERP. If the signal-to-noise ratio is comparable across signals, then the rate of decay, τ, should not vary across signals. If the timing of selection varies across signals, then the asymptote, ST_{min}, should vary across signals, despite similar rates of decay.

RESULTS

Behavior

Two monkeys searched for a red or green target stimulus among one, three, or seven distractors of the opposite color (Fig. 1*A*). Both monkeys exhibited behavioral hallmarks of efficient, pop-out visual search. The slopes of RT by set size (i.e., search slopes) were shallow for both monkeys (Fig. 1*C* and Table 1). These search slopes are characteristic of pop-out search in humans (Wolfe 1998) and monkeys (Bichot and Schall 1999). We compared our new, efficient search data with previously published data from the same monkeys performing an inefficient search task for a T among Ls and vice versa (Fig. 1*B*) (Cohen et al. 2009b). Both monkeys' search slopes were significantly shallower during efficient search (Fig. 1*C* and Table 1), and during efficient search, the slope of percent correct by set size was not significant for *monkey Q* (0.001 ± 0.002; $P = 0.43$, Wilcoxon rank sum test) and *monkey S* (−0.004 ± 0.005; $P = 0.72$). These results clearly indicate more efficient processing during pop-out search and demonstrate the low attentional demands of the task. It is the neural basis of this difference in processing efficiency that we turn to next.

Selection Time

We recorded 102 FEF neurons (48 from *monkey S* and 54 from *monkey Q*) that exhibited discharge-rate modulations following stimulus presentation or around the time of saccade initiation. This report focuses on the subset of 65/102 neurons (64%) that exhibited spatially tuned visual responses. We also recorded LFPs from 141 sites (60 in *monkey S* and 81 in *monkey Q*). Of these, 109/141 (77%) exhibited spatially tuned visual responses. The neurons and LFP sites were verified to be in FEF, based on low-threshold microstimulation (Bruce et al. 1985). During all of these recordings, we simultaneously recorded the m-N2pc from EEG electrodes over the posterior lateral cortex (Fig. 2).

Table 1. *Response time and selection time search slopes in milliseconds/items for each neural signal during efficient (pop-out) and inefficient visual search*

	Monkey Q	Monkey S
Response time		
Inefficient	22.6 ± 1.6*] *	10.5 ± 1.4*] *
Efficient	2.3 ± 0.8†] *	0.7 ± 1.0] *
FEF single units		
Inefficient	4.6 ± 1.5*] *	5.3 ± 1.7*
Efficient	1.2 ± 1.1] *	2.3 ± 1.1
FEF LFP		
Inefficient	8.2 ± 1.4*] *	6.3 ± 1.3*] *
Efficient	1.1 ± 1.0] *	0.4 ± 1.5] *
m-N2pc		
Inefficient	9.7 ± 0.5*] *	6.2 ± 0.9*
Efficient	0.9 ± 1.0] *	1.0 ± 0.9

Values are slope of linear regression ± SE. *$P < 0.001$ and †$P < 0.05$ indicate significant slope coefficient for set size. Pairwise comparisons indicate significant interaction term for set size and task. Inefficient search data have been described previously (Cohen et al. 2009a). FEF, frontal eye field; LFP, local field potential; m-N2pc, macaque homologue of the human N2pc component.

We compared the selection time—the time when each signal first reliably signaled the target location—in FEF single units, FEF LFPs, and the m-N2pc. Figure 2 shows a representative session of simultaneously recorded FEF single-unit spikes, FEF LFPs, and the m-N2pc. All three signals show an initial visual response regardless of the target's location in the visual field. However, each signal evolves over time to discriminate the location of the target stimulus before the saccade is executed. In our example session, the neuron signaled the target location with an elevated firing rate when the target is inside of the RF relative to when it is outside of the RF (165 ms after the presentation of the search array; Fig. 2*A*). The LFP recorded from the same electrode signaled the target location with a greater negativity for the target relative to distractors at approximately the same time (161 ms; Fig. 2*B*). The m-N2pc signaled the target location with a greater positivity contralateral to the target, but this selection did not occur until well after selection by both FEF spikes and LFP (179 ms; Fig. 2*C*).

Figure 3 shows the distribution of selection times for all three signals across our sample of all FEF neurons, FEF LFPs, and concurrently recorded m-N2pc. Overall, the m-N2pc selected the target later (mean ± SE, 184 ± 3.6 ms) than FEF single-unit spikes (157 ± 3.4 ms; $P < 0.001$, Wilcoxon rank sum test) and FEF LFPs (163 ± 3.3 ms; $P < 0.001$; Table 2). This chronology was also observed when these monkeys performed an inefficient T vs. L search task (Cohen et al. 2009a), but average selection time was later in all three signals (single units: 167 ± 3.6 ms, $P = 0.05$; LFP: 194 ± 3.2, $P < 0.001$; m-N2pc: 202 ± 1.9 ms, $P < 0.001$). In general, the selection

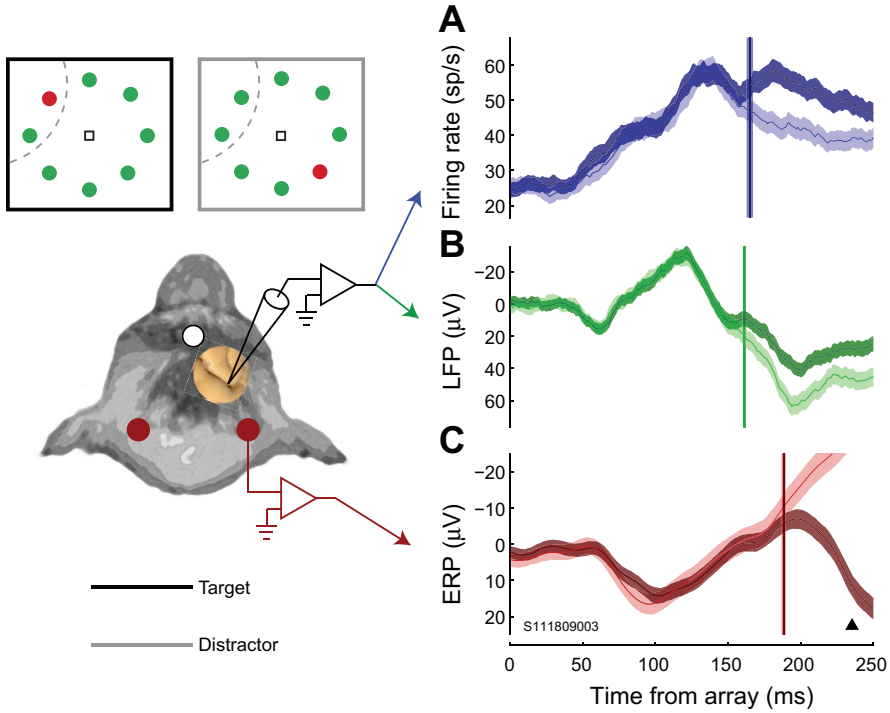

Fig. 2. Target selection during a representative session. Average activity of single unit (*A*), local field potential (LFP) site (*B*), and event-related potential (ERP) over visual cortex (*C*) when the search target was inside (dark) and opposite (light) the receptive field (or preferred location) of the signal. Bands around average activity indicate 95% confidence intervals. Vertical lines indicate selection time when the 2 curves became significantly different. Bands around selection time indicate SE estimated using a bootstrap procedure (100 samples). Solid triangle indicates mean RT for this session. sp/s, spikes/s.

time difference between FEF and the m-N2pc was smaller in *monkey Q* than *monkey S* (Table 2). One possible explanation is that FEF feedback was integrated and processed more efficiently in the visual cortex of *monkey Q*, which could explain his superior behavioral performance (mean RT: 223 ± 3.0 ms; percent correct: 97 ± 0.7%) relative to *monkey S* (mean RT: 254 ± 4.2 ms; percent correct: 83 ± 0.1%) and larger-amplitude m-N2pc (4.0 ± 0.47 μV) relative to *monkey S* (1.9 ± 0.65 μV). Regardless, it is clear that the m-N2pc never preceded selection in FEF for both monkeys, which is inconsistent with a feed-forward hypothesis. Importantly, selection took place well before mean saccadic RT, indicating that all signals selected the target sufficiently early to have played a role in the covert attention processes that precede saccade execution. Accordingly, the same pattern of results was observed when we computed selection time with all signals aligned on the time of saccade initiation; the m-N2pc selected the target significantly later (−71 ± 8.7 ms relative to saccade) than both FEF single units (−113 ± 7.9 ms; $P < 0.01$) and LFP (−105 ± 6.0 ms; $P < 0.01$).

Figure 4, *A* and *B*, shows that the simultaneously recorded FEF single units and LFPs typically selected the target before the m-N2pc (Table 2). The average difference between the FEF single-unit selection time and m-N2pc selection time was 23 ± 3.4 ms ($P < 0.001$, Wilcoxon signed rank test). The average difference between FEF LFP and m-N2pc selection time was 16 ± 2.5 ms ($P < 0.001$). When we recomputed selection time using a running millisecond-by-millisecond ANOVA (Monosov et al. 2008), the difference between the m-N2pc and FEF single units and LFPs remained positive and significant ($P < 0.001$), indicating that this result cannot be due to our selection of preferred locations for each signal. This sequence of selection supports the hypothesis that feedback from FEF contrib-

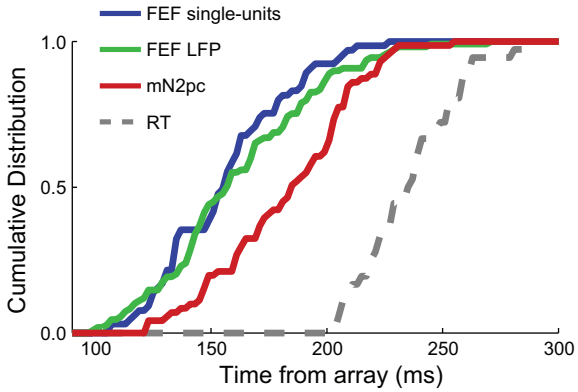

Fig. 3. Population selection times for each type of signal. Cumulative distributions of selection times measured from intracranial frontal eye field (FEF) single-unit spiking (blue), FEF LFPs (green), and the posterior macaque homologue of the human N2pc component (m-N2pc; red) during pop-out search. Selection precedes saccadic RT (dashed gray line).

Table 2. *Comparisons of target selection time and latency of visual onset across signals during efficient (pop-out) search*

	Monkey Q	Monkey S
Visual onset time, ms		
Single units	71 ± 3.8 *	66 ± 2.6 †
LFP	52 ± 1.9 *	61 ± 2.6 †
ERP	67 ± 3.1	68 ± 4.6
Selection time, ms		
Single units	155 ± 4.2 †	160 ± 5.6 *
LFP	160 ± 3.7	167 ± 6.1 *
ERP	168 ± 4.1	203 ± 4.2
Selection time difference		
ERP − single units	9 ± 4.3	39 ± 4.6*
ERP − LFP	6 ± 2.6†	31 ± 4.7*
LFP − single units	3 ± 3.2	8 ± 4.6

Values are means ± SE. Brackets with symbols indicate significant differences between signals (Wilcoxon rank sum test). Symbols alone indicate significant difference from 0 (Wilcoxon signed rank test): *$P < 0.001$; †$P < 0.05$. ERP, event-related potential.

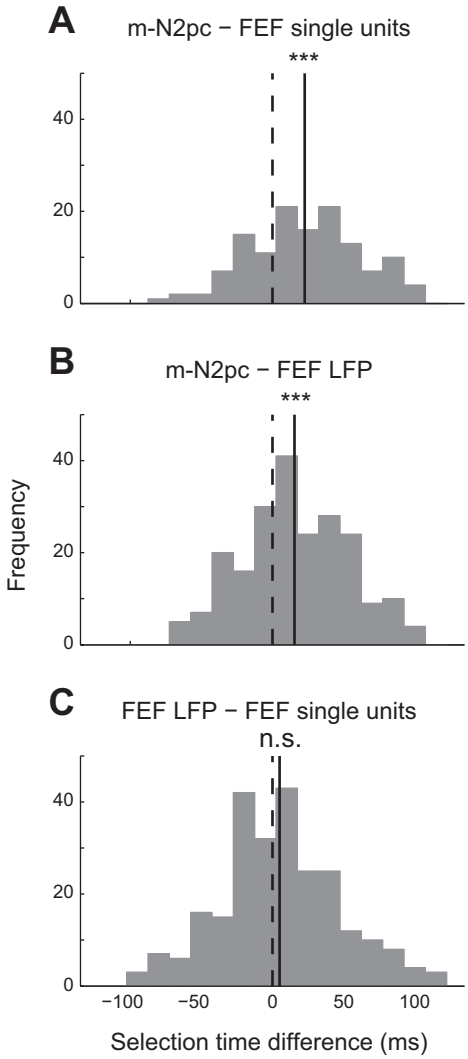

Fig. 4. Within-session selection time differences across signals. Differences between selection time measured from simultaneously recorded m-N2pc and FEF single-unit spikes (*A*), m-N2pc and FEF LFPs (*B*), and FEF LFPs and single-unit spikes (*C*). The solid, vertical line indicates the mean of the distribution. The dashed, vertical line indicates zero. ***$P < 0.001$, significant differences from 0, Wilcoxon rank sum test; n.s., nonsignificant.

utes to the generation of the m-N2pc even during pop-out search.

One potential explanation is that the m-N2pc is delayed relative to FEF, because ERPs are summing across neurons with different RFs. To test for this possibility, we also computed population selection times based on all FEF single units, LFPs, and the m-N2pc, conditionalized on whether the target was in the contralateral or ipsilateral hemifield. Analyzed in this way, all three population signals reflect summation across individual signals with different RFs within a hemisphere. Population selection times (±SE, bootstrap, 500 samples) for both FEF single units (145 ± 18) and LFPs (133 ± 15.8) were still earlier than the m-N2pc (176 ± 27). The population selection time for FEF LFP is earlier than the FEF single-unit selection time because the contralateral bias is stronger in FEF LFP than single units (Purcell et al. 2012). It is certain that the contribution of LFPs and single units to surface ERPs is more complex than simple summation across signals, but this result gives us a degree of confidence that the summation of scattered RFs alone cannot explain our results.

We also compared the relative timing of FEF single units and LFPs to assess mechanisms of efficient target selection within FEF. During inefficient search tasks, FEF single units select the target before FEF LFPs (Cohen et al. 2009a; Monosov et al. 2008). However, across the population of signals, the selection time for FEF single units and LFPs was not significantly different during efficient search (Fig. 3 and Table 2; $P = 0.40$, Wilcoxon rank sum test). Likewise, during efficient search, there was no systematic selection time difference between FEF single units and LFPs, recorded simultaneously on the same electrode (Fig. 4*C*; 0.3 ± 5.1 ms; $P = 0.5$, Wilcoxon signed rank test). We verified that the selection-time difference between FEF single units and LFP was significantly smaller during efficient search relative to inefficient search task (22 ± 3.0 ms; $P < 0.001$). This across-task difference was also evident when selection time was computed using a running ANOVA method ($P < 0.001$) (Monosov et al. 2008). These results show that when search is efficient, the FEF population activity indexed by the LFPs can discriminate the target location as rapidly as individual single units in the population.

We measured the latency of the initial visual response in each signal to ensure that the differences in selection time were not a consequence of our recording procedures. For example, maybe all electrophysiological activity is earlier when measuring high-frequency spikes or lower-frequency LFPs on the microelectrodes, relative to the surface ERPs. However, this was not the case. Across monkeys, the mean latency (±SE) of the earliest visual response in each neural signal was 68 ± 2.4 ms for FEF neurons, 56 ± 1.6 ms for FEF LFPs, and 68 ± 2.7 ms for the initial visual ERP component (Table 2). These values are consistent with recent reports (Cohen et al. 2009a; Monosov et al. 2008; Pouget et al. 2005). The visual latency of the FEF LFPs was significantly earlier than both FEF neurons and the posterior ERPs ($P < 0.001$, Wilcoxon rank sum test), but the mean latency of FEF neurons and posterior ERPs was statistically indistinguishable. The latency of FEF single units is likely similar to the N2pc, because the latency of visual responses in FEF is similar to the visual latency of neurons in extrastriate (Schmolesky et al. 1998) and posterior parietal (Andersen et al. 1987) areas thought to contain the electrical fields that directly generate the N2pc. We also computed the selection time during the memory-guided saccade task to ensure that the selection time in the m-N2pc does not consistently trail FEF activity. During the memory-guided saccade task, the mean (±SE) selection time for the m-N2pc (101 ± 3.1 ms) was not significantly different than the selection time for FEF single units (105 ± 3.9 ms; $P = 0.94$, Wilcoxon rank sum test) or LFP (111 ± 4.1 ms; $P = 0.55$), which indicates that selection time differences are specific to the visual search task.

Timing and Magnitude of Selection During Efficient and Inefficient Search

Previous studies have shown that discrimination of a target from distractors by visually responsive FEF neurons marks the outcome of visual processing for attentional selection [e.g., Sato and Schall (2003); Thompson et al. (1996, 1997)]. During inefficient search, selection time increases with set size in FEF

neurons, LFPs, and the m-N2pc (Bichot et al. 2001b; Cohen et al. 2009a, b; Sato et al. 2001), which is consistent with delays in the time required to reliably focus attention on the target. Essentially, all models of visual attention propose that distractors do not effectively compete for selection during pop-out search [e.g., Duncan and Humphreys (1989); Treisman and Sato (1990); Wolfe (2007)]. Therefore, if selection time represents an index of attentional allocation, then we would expect it to remain invariant over set size when search is efficient, and the target pops out. Indeed, we found that the mean (±SE) slope of selection time by set size during efficient search was not significant for FEF neurons (1.7 ± 1.02 ms/item; $P = 0.09$), FEF LFP (0.6 ± 0.87 μV/item; $P = 0.48$), and m-N2pc (0.9 ± 0.9 μV/item; $P = 0.32$; linear regression; Fig. 5 and Table 1). This contrasts sharply with the significant increases in selection time observed during inefficient search for all three signals (FEF single-units: 4.9 ± 1.14 ms/item, $P < 0.001$; FEF LFP: 7.3 ± 0.96 μV/item, $P < 0.001$; m-N2pc: 3.3 ± 0.49 μV/item, $P < 0.001$) (Cohen et al. 2009a). The difference in slope of selection time by set size for inefficient search relative to efficient search was significant for all three signals (all $P < 0.001$). This result indicates that selection time increases with the attentional demands of the search task and not simply the number of objects in the visual field.

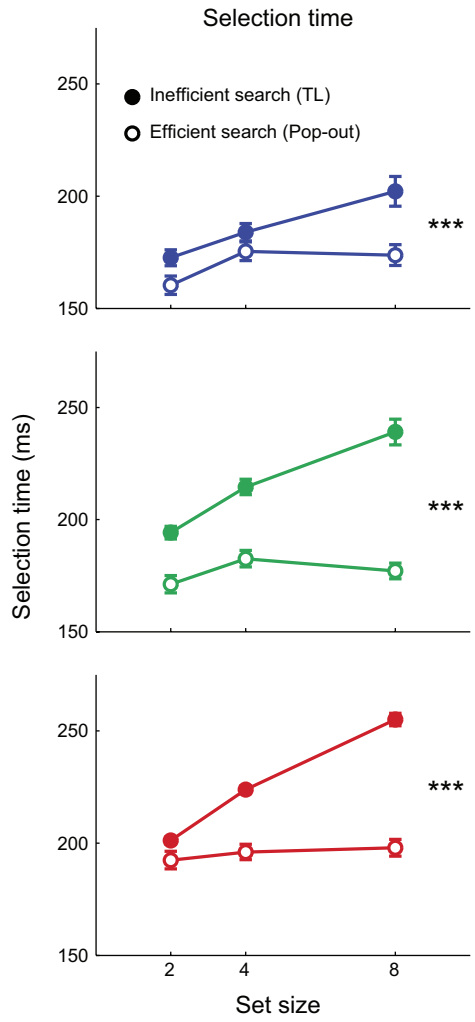

Fig. 5. Average selection time for FEF single-unit spikes (*top*), FEF LFPs (*middle*), and m-N2pc (*bottom*) at each set size. ***$P < 0.001$, significant difference in slope across efficient (pop-out) and inefficient (T vs. L) search (multiple linear regression). Error bars indicate SE.

Previous studies have also found that the amplitude of the N2pc (Luck et al. 1997b; Luck and Hillyard 1990, 1994a) and FEF neurons (Bichot and Schall 1999; Cohen et al. 2009b) depends on attentional demands. During inefficient search, the amplitude of the m-N2pc (Woodman et al. 2007) and FEF neurons (Cohen et al. 2009b) declines with set size. The amplitude of ERP components is related to the variability in the latency (Luck 2005); greater amplitude is expected with lower latency variability, and lower amplitude is expected with greater latency variability. Thus if the latency of the N2pc truly reflects an index of attentional allocation, amplitude should decline with set size during inefficient search when selection-time variability increases but should remain constant with set size during pop-out when selection-time variability is constant. We might also expect reductions in the magnitude of the N2pc, because the magnitude of discrimination in extrastriate neurons decreases with target salience [e.g., Katsuki and Constantinidis (2012)]. Indeed, we found that the slope of amplitude by set size during efficient search was not significantly different from zero for FEF single units (0.01 ± 0.27 spikes·s^{-1}·item^{-1}), FEF LFP (−0.01 ± 0.16 μV/item), and m-N2pc (0.04 ± 0.13 μV/item; all $P > 0.05$; Fig. 6). In contrast, the average slope of amplitude by set size during inefficient search significantly declined for FEF single units (−0.59 ± 0.30 spikes·s^{-1}·item^{-1}; $P < 0.05$), FEF LFP (−0.35 ± 0.13; $P < 0.001$), and m-N2pc (−0.19 ± 0.04; $P < 0.001$). This resulted in a significantly smaller magnitude of selection for FEF LFPs and m-N2pc during inefficient search (LFPs: 3.0 ± 0.56 μV; m-N2pc: 2.2 ± 0.15 μV) relative to efficient search (LFPs: 5.1 ± 0.65 μV, $P < 0.01$; m-N2pc: 3.4 ± 0.47 μV, $P < 0.01$, Wilcoxon rank sum test). This pattern of modulation is very similar to effects seen in the human N2pc (Eimer 1996; Luck and Hillyard 1990).

We used a bootstrapping procedure to test whether the reductions in human N2pc amplitude with set size during inefficient search were due to increases in selection-time variability. We randomly sampled, with replacement, from all trials recorded during each set size condition and computed the selection time for the m-N2pc for this subset of trials. The sample size was matched across conditions. This process was repeated 50 times, and the SD of selection time across samples was used as an index of selection-time variability within that condition. With the use of this procedure, we found that selection-time variability was relatively constant during pop-out search (set size 2: SD = 28; set size 4: SD = 27; set size 8: SD = 28) but increased during inefficient (T vs. L) search (set size 2: SD = 25; set size 4: SD = 31; set size 8: SD = 42). This result suggests that increased variability in selection time is at least one contributing factor to reductions in the amplitude of the m-N2pc during inefficient search. Altogether, these results indicate that selection time and amplitude in FEF neurons are sensitive to attentional demands and extend these observations to LFPs and m-N2pc.

Trial-by-Trial Correlation of Spike Rate, LFP, and ERP Amplitude

The similar pattern of modulation in all three signals suggests that FEF may be one source of modulations in posterior visual areas that generates the N2pc. If feedback from FEF is

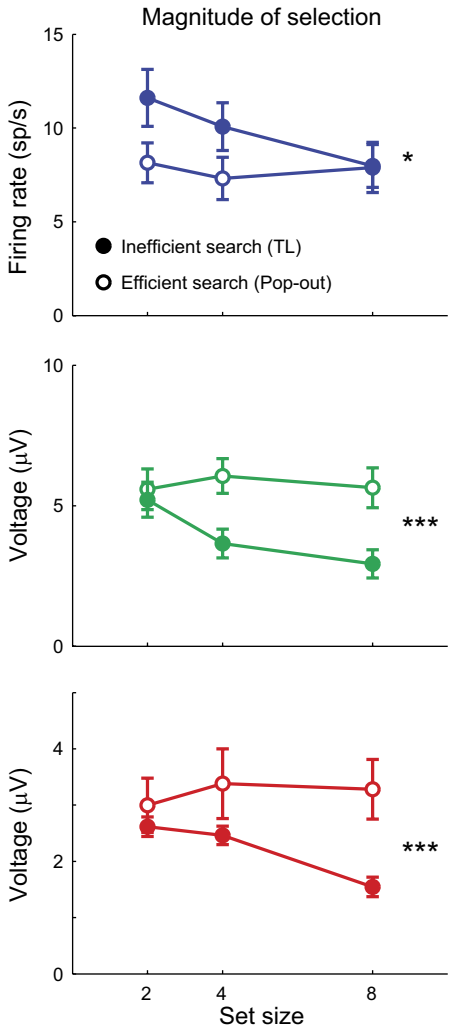

Fig. 6. Average magnitude of selection (response amplitude when the target was in the preferred location of the signal minus the response amplitude when a distractor was in the preferred location) for FEF single-unit spikes (*top*), FEF LFPs (*middle*), and m-N2pc (*bottom*) at each set size. $*P < 0.05$; $***P < 0.001$, significant difference in slope across efficient (pop-out) and inefficient (T vs. L) search (multiple linear regression). Error bars indicate SE.

present during pop-out search and influences the neural mechanisms that generate the m-N2pc, then the trial-by-trial amplitude of FEF LFPs should covary with posterior ERP amplitude. The mean correlation between FEF LFP and m-N2pc was significantly greater than zero (0.53 ± 0.02; $P < 0.001$, Wilcoxon signed rank test) and comparable with values observed during inefficient search (Cohen et al. 2009a). We verified that the correlation remained significant when performed on the difference in amplitude between posterior surface electrodes (Fig. 7*A*; $r = 0.03 \pm 0.009$; $P < 0.01$), which rules out the possibility that it is simply due to shared noise at the reference. Moreover, this correlation was absent during the baseline period before array presentation ($P = 0.46$) and when only distractors were in the RF of the LFP ($P = 0.20$), illustrating both spatial and temporal specificity. It is known that only the superficial layers of FEF feed back to visual cortex (Pouget et al. 2009), which is a likely reason why some LFP sites show negligible correlations with m-N2pc (Fig. 7*A*). Whereas it is possible that this correlation could be due to either feedforward or feedback signals, our observation that selection emerges first in FEF suggests that it reflects feedback. This interpretation is supported by studies showing a causal effect of microstimulation and pharamacological inactivation of FEF on neuronal activity in posterior visual areas (Ekstrom et al. 2008; Monosov et al. 2011; Moore and Armstrong 2003).

The spike rates of FEF single units were significantly correlated with LFPs recorded from the same electrode (Fig. 7*B*; $r = -0.09 \pm 0.008$; $P < 0.001$), which is consistent with the hypothesis that LFPs reflect postsynaptic activity of neurons surrounding the electrode tip. This correlation dropped but remained significant when it was performed across electrodes spaced ~1 mm apart ($r = -0.02 \pm 0.008$; $P < 0.001$), suggesting that these units were nearing the edge of the area over which the LFP integrated (Katzner et al. 2009). In contrast, the mean correlation between FEF spiking and m-N2pc, measured at posterior ERP electrodes, was not significantly different from zero (Fig. 7*C*; $r = 0.004$, $P = 0.61$), which is consistent with studies showing a negligible relationship between these electrophysiological signals (Cohen et al. 2009a).

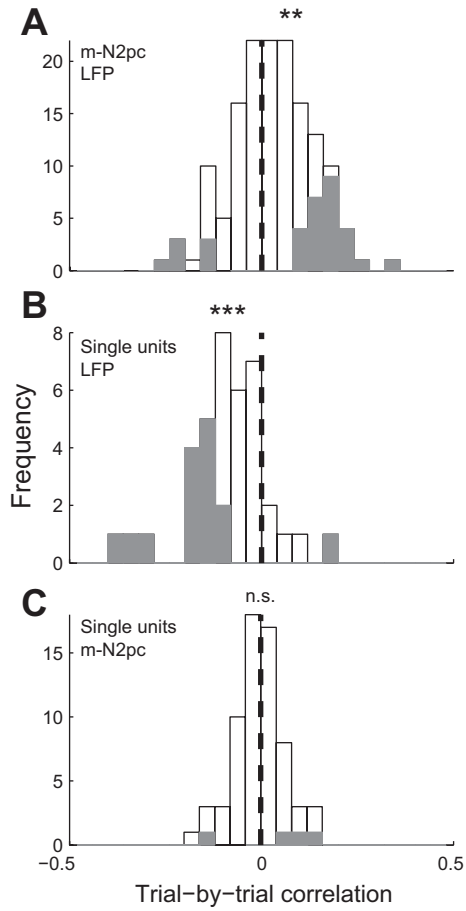

Fig. 7. Trial-by-trial correlations between FEF LFP amplitude and the amplitude difference between posterior EEG electrodes (*A*), between FEF LFP amplitude and FEF single-unit firing rate recorded on the same electrode (*B*), and between FEF single-unit firing rate and the amplitude difference between posterior EEG electrodes (*C*). $**P < 0.01$; $***P < 0.001$, significance from 0, indicated by the vertical, dashed lines, Wilcoxon rank sum.

Control for Differences in Signal-to-Noise Ratio Across Measures of Neural Activity

A potential concern is that the observed differences in selection time across the electrophysiological signals are due to differences in the signal-to-noise properties of each signal. The pattern of target selection times could just be a difference inherent in the neural measures at different spatial scales. In particular, the signal-to-noise characteristics of the spike times of single neurons may be different from the signal-to-noise characteristics of a LFP derived from a weighted average of $\sim 10^5$ neurons within ~ 1 mm^2 of the electrode tip (Katzner et al. 2009) and from the signal-to-noise characteristics of an ERP component derived from a weighted average of many centimeters of cortex (Nunez and Srinivasan 2006). It may be that through summation, the LFPs and ERPs become more reliable measures or the summation may introduce more noise into the LFP and ERP. Following Cohen et al. (2009a), we reasoned that the signal-to-noise characteristics of each neural signal will determine how increasing trial numbers affect the reliability with which the target can be discriminated [see also Bichot et al. (2001b)]. We fit an exponential curve to selection times as a function of trial number measured from FEF neurons, LFP, and m-N2pc. The average number of trials/session was greater than the number of trials necessary for all signals to reach asymptote (Fig. 8*A*). The rate of decay, τ, was statistically indistinguishable for neurons (101 ± 26.4; median ± SE), LFP (139 ± 33.0), and m-N2pc (129 ± 24.9; Fig. 8*B*; all $P > 0.09$, Wilcoxon rank sum test). In a previous study of inefficient search (Cohen et al. 2009a), the corresponding values were 94 ± 14.2, 144 ± 21.7, and 97 ± 17.5 for neurons, LFP, and m-N2pc, respectively (all $P > 0.14$). This result is consistent with the comparable confidence intervals that are apparent in Fig. 2. However, the level at which selection time reached asymptote was lowest for neurons (138 ± 4.3), followed by LFP (150 ± 4.2), and latest by m-N2pc (180 ± 4.0; Fig. 8*C*; all $P < 0.05$, Wilcoxon rank sum test). This result is consistent with the ordering of selection times reported above (Fig. 3). In a previous study of inefficient search (Cohen et al. 2009a), the corresponding values were 151 ± 3.2, 172 ± 5.2, and 188 ± 2.7 for neurons, LFP, and the m-N2pc, respectively (all $P < 0.01$). Thus we can conclude that the timing differences across the signals are not due to different signal-to-noise characteristics of the neural measures.

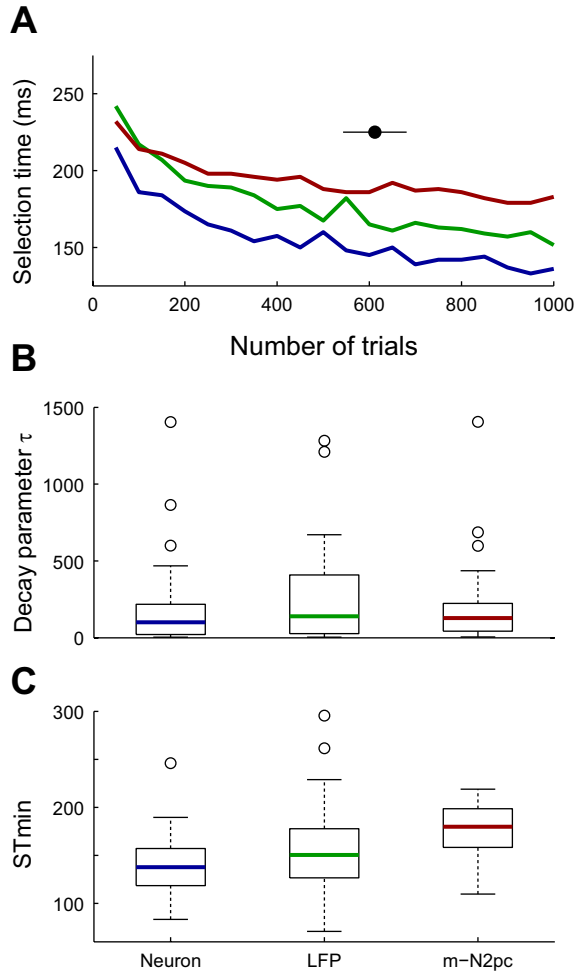

Fig. 8. Selection time by number of trials. *A*: average selection time as a function of number of trials (randomly sampled with replacement) across recordings of FEF single units (blue), LFP (green), and m-N2pc (red). The black point (with SE line) indicates the average number of trials in our data set. *B*: decay parameter (τ) estimates from exponential fits to the selection time by number of trials. *C*: asymptote parameter (ST_{min}) estimates from the exponential fits plotted in *B*. The open circles show outliers that are >1.5 times the interquartile range.

DISCUSSION

To understand the neural mechanisms that generate attention-related ERPs, we recorded the m-N2pc simultaneously with single-unit spiking and LFPs in FEF. We asked how the timing of selection in all three signals depends on the attentional demands of the task by directly comparing the timing of selection during an efficient pop-out search task with an inefficient form search task (Cohen et al. 2009a). We showed that both the timing and magnitude of selection in all three signals depend on the attentional demands of the task. However, selection was evident in FEF before the m-N2pc regardless of search efficiency. These results are consistent with the hypothesis that the primate N2pc is due to feedback from higher cortical areas, even when bottom-up salience is sufficient for task performance. These results also inform us about the neural mechanisms that generate the N2pc and constrain theories of visual attention.

Comparison of Human and m-N2pc

Before we consider the relevance of our findings to the study of human ERPs, we must first ask whether the m-N2pc indexes the same cognitive operations as the human N2pc. The m-N2pc satisfies several established criteria for across-species homology (Woodman 2011). Previous studies have shown that the spatial distribution of the N2pc is maximal over posterior electrodes in both humans (Luck and Hillyard 1994a) and monkeys (Cohen et al. 2009a; Woodman et al. 2007). In addition, previous studies have found that the latency of the N2pc increases with set size in both humans (Luck and Hillyard 1990) and monkeys (Woodman et al. 2007) when search is inefficient. We found that the latency and amplitude of the m-N2pc are insensitive to changes in set size during efficient pop-out search, which is consistent with an index of attentional demands and not simply the number of objects on the screen.

We also found that the amplitude of the m-N2pc is greatest during efficient search, which is observed with the human N2pc (Eimer 1996). Thus the m-N2pc satisfies multiple criteria for homology, including a similar spatial distribution, task dependence, and timing. Our findings provide new support for this across-species homology.

One notable across-species difference is that the polarity of the N2pc is reversed. Humans show a contralateral negativity, and monkeys show a contralateral positivity. This is likely due to differences in cortical folding in posterior visual areas across the species. For example, macaque V4 is located on the surface of the prelunate gyrus (Zeki 1971), but the human homologue spans several sulci (Orban et al. 2004). Another potential across-species difference is that several studies of the human N2pc have reported increases in amplitude with attentional demands (Hopf et al. 2002; Luck et al. 1997b), whereas we observed declines in the m-N2pc. This is likely due to differences in task design rather than species. In humans, this effect is observed when targets and distractors are tightly grouped in a limited portion of the visual field. In contrast, when stimuli are well spaced across hemifields, as in our monkey studies, amplitude decreases with additional stimuli (Eimer 1996). Future experiments that compare the N2pc observed in humans and monkeys under identical experimental design [e.g., Godlove et al. (2011a); Reinhart et al. (2012a, b)] can further establish the homology across species.

The Origin and Interpretation of the N2pc

We found that the pattern of modulation in FEF LFP and N2pc was similar during inefficient and efficient visual search, and the signals were correlated on a trial-by-trial basis. This suggests that FEF is influencing the generation of the N2pc, but it seems unlikely that the contribution is direct. First, voltage distributions, current source density topography, and dipole source modeling suggest that the dipole seen as the N2pc on the scalp originates in the posterior visual cortex in humans (Hopf et al. 2000, 2004; Luck et al. 1997a) and monkeys (Cohen et al. 2009a; Woodman et al. 2007; Young et al. 2011). Second, the timing differences that we observed seem inconsistent with identification of FEF as the direct neural generator, because extracranial EEG is not delayed relative to intracranial synaptic activity (Givre et al. 1994; Nunez and Srinivasan 2006). However, both the human N2pc and the m-N2pc are not observed at anterior electrodes near FEF (Cohen et al. 2009a; Woodman et al. 2007). How can this be? Two possibilities are consistent with what we assume is occurring in the working brain. First, the electrical fields generated in the FEF might actively be canceled by electric fields of the opposite polarity in nearby cortical areas. Second, it is possible that the dipole is simply oriented parallel to the skull, such that it does not produce an observable extracranial signal. Future recordings from multiple intracranial electrodes will provide more detailed information about the configuration of the electrical fields in the prefrontal cortex and distinguish between these explanations.

Instead, these observations are consistent with the hypothesis that FEF is part of a frontal-parietal network involved in driving attentional shifts in posterior visual areas thought to generate the m-N2pc (Corbetta 1998). FEF is part of a distributed network of structures shown to encode a representation of visual salience for guiding attentional deployments (Thompson and Bichot 2005). Our observation that activity in FEF modulates concurrently with the m-N2pc during both efficient and inefficient search suggests that this network is engaged regardless of search efficiency. Some studies have questioned the need for an influence of frontal structures during efficient search tasks based on functional MRI (fMRI) responses (Leonards et al. 2000) and effects of transcranial magnetic stimulation (Muggleton et al. 2003) in prefrontal areas during inefficient but not efficient search. However, these results are inconsistent with findings from monkey studies showing that reversible inactivation of FEF with the GABA agonist muscimol impairs performance on pop-out search tasks (Monosov and Thompson 2009; Wardak et al. 2006). In addition, other studies report comparable fMRI activation in human (Anderson et al. 2007) and monkey (Wardak et al. 2010) FEF, irrespective of search efficiency. Thus our results add to converging evidence suggesting that FEF plays an important role in processing visual targets even during efficient search tasks.

Our results also inform the interpretation of the cognitive processes indexed by the primate N2pc. The degree to which the human N2pc reflects the initial spatial selection of a target or postselection processing has been unclear (Eimer and Kiss 2010; Theeuwes 2010). Our data place clear limits on the degree to which the latency of the N2pc can be interpreted as the time of initial spatial selection, because the N2pc followed selection in prefrontal cortex even during an efficient search task that required minimal feature analysis. One limitation of the current task design is that the singleton was always task relevant, and therefore, we cannot make strong claims about the relative timing of selectivity based on pure bottom-up physical salience. However, our results are consistent with a growing body of work demonstrating the sensitivity of the N2pc to top-down factors and extend that work by suggesting that FEF is a likely source of this top-down modulation. When a color singleton is not task relevant, the N2pc is small or absent (Eimer et al. 2009; Luck and Hillyard 1994a), and selectivity in FEF is minimal (Bichot et al. 2001a). The N2pc is also sensitive to rewards associated with target localization and identification (Kiss et al. 2009), as are FEF neurons (Ding and Hikosaka 2006). Lastly, trial history and experience influence both the N2pc (An et al. 2012; Eimer et al. 2010) and FEF neurons (Bichot and Schall 1999, 2002; Bichot et al. 1996). The same FEF neurons that are modulated by these top-down factors project to earlier visual areas thought to generate the N2pc (Pouget et al. 2009), which is consistent with the hypothesis that FEF is the source of these modulations.

Relation to Previous Studies of Attentional Selection Across Cortex

Several recent studies have investigated the timing of attentional selection across cortex using paired intracranial recordings. Zhou and Desimone (2011) observed earlier selection in FEF neurons relative to V4 neurons during inefficient conjunction search tasks. Similarly, during inefficient conjunction search, Buschman and Miller (2007) observed earlier selection in FEF and dorsolateral prefrontal neurons. In addition, Monosov et al. (2010) found that FEF neurons exhibited significant spatial selectivity before IT neurons exhibited significant ob-

ject selectivity during a difficult search and identification task. Thus converging evidence supports the hypothesis that attentional selection in FEF neurons precedes attentional selection in several earlier visual areas when tasks are attentionally demanding [see also Cohen et al. (2009a)], but findings during efficient pop-out search are less consistent. One study found that selectivity in the lateral intraparietal area precedes selectivity in FEF and the dorsolateral prefrontal cortex during pop-out search (Buschman and Miller 2007), but a recent study found the opposite—frontal areas selected before parietal areas during pop-out (Katsuki and Constantinidis 2012). In addition, studies using nearly identical task designs and analytical methods found that both FEF and LIP select the location of a color singleton at approximately the same time (Thomas and Pare 2007; Thompson et al. 1996). Our observation that the m-N2pc selects the target location later than FEF is consistent with studies suggesting that FEF selectivity precedes selectivity in early visual areas, but it is important to note that ERPs cannot be regarded as a direct proxy for underlying neural activity. ERPs are thought to reflect the summation of synchronous activity across many centimeters of cortex (Nunez and Srinivasan 2006), and the N2pc likely reflects attentional selection across multiple visual areas. Thus additional simultaneous recordings in frontal and parietal areas will be necessary to conclusively determine the degree to which the timing of selection across neurons in different cortical areas depends on task demands.

In addition to our observations regarding the timing relationship between FEF and m-N2pc, we observed differences in the relative timing of selection in FEF single units and LFP depending on the attentional demands of the task. Previous studies have found that FEF LFPs select the target later than FEF single units (Cohen et al. 2009a; Monosov et al. 2008). We found that the delay in selection time between FEF single units and LFPs was absent during pop-out. LFPs reflect the synaptic activity of thousands of neurons surrounding the electrode tip (Katzner et al. 2009; Mitzdorf 1985), whereas spiking activity reflects only a single neuron. Therefore, one interpretation of this result is that the population of FEF neurons contributing to the LFP reached a consensus about target identity more efficiently during pop out. The absence of a delay between selection in FEF single units and LFP was unexpected given a previous report showing a significant delay between the two signals in one monkey performing a covert pop-out search task in which the target location was reported via a lever turn (Monosov et al. 2008). Covert visual search requires active suppression of saccade-generating neurons in FEF (Thompson et al. 2005), which could have postponed LFP selectivity. In line with the present findings, another interpretation is that the delayed LFP selection time relative to single units during covert search reflects the increased attentional demands required to map the target location to the lever turn.

Relation to Theories of Visual Search and Attention

Early models of visual attention proposed that targets that could be distinguished by a single feature could be localized "pre-attentively", solely through bottom-up selection of local feature differences (Itti and Koch 2001; Treisman and Gelade 1980). Other studies have shown that prior knowledge and expectation have a strong influence on pop-out performance (Joseph et al. 1997; Maljkovic and Nakayama 1994; Treisman and Gormican 1988). Our finding that an attentional control area, FEF, contributes to the generation of the N2pc during efficient search is consistent with theories of visual attention that propose no strong dichotomy between efficient and inefficient search (Bundesen et al. 2005; Desimone and Duncan 1995; Treisman and Sato 1990; Wolfe 2007). This result is consistent with a recent study that found that the enhanced response of V4 neurons to a pop-out stimulus is eliminated when attention is directed elsewhere in the visual field (Burrows and Moore 2009). Thus our findings add to behavioral and neurophysiological evidence that top-down input from the frontal cortex may guide attentional selection even during pop-out search.

ACKNOWLEDGMENTS

We thank J. Cohen and R. Heitz for collecting the inefficient search data.

GRANTS

This work was supported by National Eye Institute Grants T32-EY07135, R01-EY019882, R01-EY08890, and P30-EY008126; National Institute of Child Health and Human Development Grant P30-HD015052; and Robin and Richard Patton through the E. Bronson Ingram Chair in Neuroscience.

DISCLOSURES

No conflicts of interest, financial or otherwise, are declared by the authors.

AUTHOR CONTRIBUTIONS

Author contributions: B.A.P., J.D.S., and G.F.W. conception and design of research; B.A.P. performed experiments; B.A.P. analyzed data; B.A.P., J.D.S., and G.F.W. interpreted results of experiments; B.A.P. prepared figures; B.A.P. drafted manuscript; B.A.P., J.D.S., and G.F.W. edited and revised manuscript; B.A.P., J.D.S., and G.F.W. approved final version of manuscript.

REFERENCES

An A, Sun M, Wang Y, Wang F, Ding Y, Song Y. The N2pc is increased by perceptual learning but is unnecessary for the transfer of learning. *PLoS One* 7: e34826, 2012.

Andersen RA, Essick GK, Siegel RM. Neurons of area 7 activated by both visual stimuli and oculomotor behavior. *Exp Brain Res* 67: 316–322, 1987.

Anderson EJ, Mannan SK, Husain M, Rees G, Sumner P, Mort DJ, McRobbie D, Kennard C. Involvement of prefrontal cortex in visual search. *Exp Brain Res* 180: 289–302, 2007.

Anderson JC, Kennedy H, Martin KAC. Pathways of attention: synaptic relationships of frontal eye field to V4, lateral intraparietal cortex, and area 46 in macaque monkey. *J Neurosci* 31: 10872–10881, 2011.

Bichot NP, Rao SC, Schall JD. Continuous processing in macaque frontal cortex during visual search. *Neuropsychologia* 39: 972–982, 2001a.

Bichot NP, Schall JD. Effects of similarity and history on neural mechanisms of visual selection. *Nat Neurosci* 2: 549–554, 1999.

Bichot NP, Schall JD. Priming in macaque frontal cortex during popout visual search: feature-based facilitation and location-based inhibition of return. *J Neurosci* 22: 4675–4685, 2002.

Bichot NP, Schall JD, Thompson KG. Visual feature selectivity in frontal eye fields induced by experience in mature macaques. *Nature* 381: 697–699, 1996.

Bichot NP, Thompson KG, Rao SC, Schall JD. Reliability of macaque frontal eye field neurons signaling saccade targets during visual search. *J Neurosci* 21: 713–725, 2001b.

Boehler CN, Tsotsos JK, Schoenfeld MA, Heinze HJ, Hopf JM. Neural mechanisms of surround attenuation and distractor competition in visual search. *J Neurosci* 31: 5213–5224, 2011.

Britten KH, Shadlen MN, Newsome WT, Movshon JA. The analysis of visual motion: a comparison of neuronal and psychophysical performance. *J Neurosci* 12: 4745–4765, 1992.

Bruce CJ, Goldberg ME. Primate frontal eye fields. I. Single neurons discharging before saccades. *J Neurophysiol* 53: 603–635, 1985.

Bruce CJ, Goldberg ME, Bushnell MC, Stanton GB. Primate frontal eye fields. II. Physiological and anatomical correlates of electrically evoked eye movements. *J Neurophysiol* 54: 714–734, 1985.

Bundesen C, Habekost T, Kyllingsbæk S. A neural theory of visual attention: bridging cognition and neurophysiology. *Psychol Rev* 112: 291–328, 2005.

Burrows BE, Moore T. Influence and limitations of popout in the selection of salient visual stimuli by area V4 neurons. *J Neurosci* 29: 15169–15177, 2009.

Buschman TJ, Miller EK. Top-down versus bottom-up control of attention in the prefrontal and posterior parietal cortices. *Science* 315: 1860–1862, 2007.

Cohen JY, Heitz RP, Schall JD, Woodman GF. On the origin of event-related potentials indexing covert attentional selection during visual search. *J Neurophysiol* 102: 2375–2386, 2009a.

Cohen JY, Heitz RP, Woodman GF, Schall JD. Neural basis of the set-size effect in frontal eye field: timing of attention during visual search. *J Neurophysiol* 101: 1699–1704, 2009b.

Corbetta M. Frontoparietal cortical networks for directing attention and the eye to visual locations: identical, independent, or overlapping neural systems? *Proc Natl Acad Sci USA* 95: 831–838, 1998.

Desimone R, Duncan J. Neural mechanisms of selective visual attention. *Annu Rev Neurosci* 18: 193–222, 1995.

Ding L, Hikosaka O. Comparison of reward modulation in the frontal eye field and caudate of the macaque. *J Neurosci* 26: 6695–6703, 2006.

Duncan J, Humphreys GW. Visual search and stimulus similarity. *Psychol Rev* 96: 433–458, 1989.

Eimer M. The N2pc component as an indicator of attentional selectivity. *Electroencephalogr Clin Neurophysiol* 99: 225–234, 1996.

Eimer M, Kiss M. The top-down control of visual selection and how it is linked to the N2pc component. *Acta Psychol (Amst)* 135: 100–102, 2010.

Eimer M, Kiss M, Cheung T. Priming of pop-out modulates attentional target selection in visual search: behavioural and electrophysiological evidence. *Vision Res* 50: 1353–1361, 2010.

Eimer M, Kiss M, Press C, Sauter D. The roles of feature-specific task set and bottom-up salience in attentional capture: an ERP study. *J Exp Psychol Hum Percept Perform* 35: 1316–1328, 2009.

Ekstrom LB, Roelfsema PR, Arsenault JT, Bonmassar G, Vanduffel W. Bottom-up dependent gating of frontal signals in early visual cortex. *Science* 321: 414–417, 2008.

Givre SJ, Schroeder CE, Arezzo JC. Contribution of extrastriate area V4 to the surface-recorded flash VEP in the awake macaque. *Vision Res* 34: 415–428, 1994.

Godlove DC, Emeric EE, Segovis CM, Young MS, Schall JD, Woodman GF. Event-related potentials elicited by errors during the stop-signal task. I. Macaque monkeys. *J Neurosci* 31: 15640–15649, 2011a.

Godlove DC, Garr AK, Woodman GF, Schall JD. Measurement of the extraocular spike potential during saccade countermanding. *J Neurophysiol* 106: 104–114, 2011b.

Gregoriou GG, Gotts SJ, Desimone R. Cell-type-specific synchronization of neural activity in FEF with V4 during attention. *Neuron* 73: 581–594, 2012.

Heitz RP, Cohen JY, Woodman GF, Schall JD. Neural correlates of correct and errant attentional selection revealed through N2pc and frontal eye field activity. *J Neurophysiol* 104: 2433–2441, 2010.

Helmholtz H. Ueber einige Gesetze der Vertheilung elektrischer Ströme in körperlichen Leitern mit Anwendung auf die thierisch-elektrischen Versuche. *Annalen der Physik* 165: 211–233, 1853.

Hickey C, McDonald JJ, Theeuwes J. Electrophysiological evidence of the capture of visual attention. *J Cogn Neurosci* 18, 604–613, 2006.

Hikosaka O, Wurtz RH. Visual and oculomotor functions of monkey substantia nigra pars reticulata. IV. Relation of substantia nigra to superior colliculus. *J Neurophysiol* 49: 1285–1301, 1983.

Hopf JM, Boelmans K, Schoenfeld AM, Heinze HJ, Luck SJ. How does attention attenuate target-distractor interference in vision? Evidence from magnetoencephalographic recordings. *Brain Res Cogn Brain Res* 15: 17–29, 2002.

Hopf JM, Boelmans K, Schoenfeld MA, Luck SJ, Heinze HJ. Attention to features precedes attention to locations in visual search: evidence from electromagnetic brain responses in humans. *J Neurosci* 24: 1822–1832, 2004.

Hopf JM, Luck SJ, Girelli M, Hagner T, Mangun GR, Scheich H, Heinze HJ. Neural sources of focused attention in visual search. *Cereb Cortex* 10: 1233–1241, 2000.

Itti L, Koch C. Computational modelling of visual attention. *Nat Rev Neurosci* 2: 194–203, 2001.

Joseph JS, Chun MM, Nakayama K. Attentional requirements in a "preattentive" feature search task. *Nature* 387: 805–807, 1997.

Katsuki F, Constantinidis C. Early involvement of prefrontal cortex in visual bottom-up attention. *Nat Neurosci* 15: 1160–1166, 2012.

Katzner S, Nauhaus I, Benucci A, Bonin V, Ringach DL, Carandini M. Local origin of field potentials in visual cortex. *Neuron* 61: 35–41, 2009.

Kiss M, Driver J, Eimer M. Reward priority of visual target singletons modulates event-related potential signatures of attentional selection. *Psychol Sci* 20: 245–251, 2009.

Leonards U, Sunaert S, Van Hecke P, Orban GA. Attention mechanisms in visual search—an fMRI study. *J Cogn Neurosci* 12: 61–75, 2000.

Luck SJ. *An Introduction to the Event-Related Potential Technique*. Cambridge, MA: MIT Press, 2005.

Luck SJ, Chelazzi L, Hillyard SA, Desimone R. Neural mechanisms of spatial selective attention in areas V1, V2, and V4 of macaque visual cortex. *J Neurophysiol* 77: 24–42, 1997a.

Luck SJ, Girelli M, McDermott MT, Ford MA. Bridging the gap between monkey neurophysiology and human perception: an ambiguity resolution theory of visual selective attention. *Cogn Psychol* 33: 64–87, 1997b.

Luck SJ, Hillyard SA. Electrophysiological correlates of feature analysis during visual search. *Psychophysiology* 31: 291–308, 1994a.

Luck SJ, Hillyard SA. Electrophysiological evidence for parallel and serial processing during visual search. *Percept Psychophys* 48: 603–617, 1990.

Luck SJ, Hillyard SA. Spatial filtering during visual search: evidence from human electrophysiology. *J Exp Psychol Hum Percept Perform* 20: 1000–1014, 1994b.

Maljkovic V, Nakayama K. Priming of pop-out: I. Role of features. *Mem Cognit* 22: 657–672, 1994.

Mitzdorf U. Current source-density method and application in cat cerebral cortex: investigation of evoked potentials and EEG phenomena. *Physiol Rev* 65: 37–100, 1985.

Monosov IE, Sheinberg DL, Thompson KG. Paired neuron recordings in the prefrontal and inferotemporal cortices reveal that spatial selection precedes object identification during visual search. *Proc Natl Acad Sci USA* 107: 13105–13110, 2010.

Monosov IE, Sheinberg DL, Thompson KG. The effects of prefrontal cortex inactivation on object responses of single neurons in the inferotemporal cortex during visual search. *J Neurosci* 31: 15956–15961, 2011.

Monosov IE, Thompson KG. Frontal eye field activity enhances object identification during covert visual search. *J Neurophysiol* 102: 3656–3672, 2009.

Monosov IE, Trageser JC, Thompson KG. Measurements of simultaneously recorded spiking activity and local field potentials suggest that spatial selection emerges in the frontal eye field. *Neuron* 57: 614–625, 2008.

Moore T, Armstrong KM. Selective gating of visual signals by microstimulation of frontal cortex. *Nature* 421: 370–373, 2003.

Muggleton NG, Juan CH, Cowey A, Walsh V. Human frontal eye fields and visual search. *J Neurophysiol* 89: 3340–3343, 2003.

Ninomiya T, Sawamura H, Inoue K, Takada M. Segregated pathways carrying frontally derived top-down signals to visual areas MT and V4 in macaques. *J Neurosci* 32: 6851–6858, 2011.

Nunez PL, Srinivasan R. *Electric Fields of the Brain: the Neurophysics of EEG*. Cary, NC: Oxford University Press USA, 2006.

Orban GA, Van Essen D, Vanduffel W. Comparative mapping of higher visual areas in monkeys and humans. *Trends Cogn Sci* 8: 315–324, 2004.

Pouget P, Emeric EE, Stuphorn V, Reis K, Schall JD. Chronometry of visual responses in frontal eye field, supplementary eye field, and anterior cingulate cortex. *J Neurophysiol* 94: 2086–2092, 2005.

Pouget P, Stepniewska I, Crowder EA, Leslie MW, Emeric EE, Nelson MJ, Schall JD. Visual and motor connectivity and the distribution of calcium-binding proteins in macaque frontal eye field: implications for saccade target selection. *Front Neuroanat* 3: 1–14, 2009.

Purcell BA, Weigand PK, Schall JD. Supplementary eye field during visual search: salience, cognitive control, and performance monitoring. *J Neurosci* 32: 10273–10285, 2012.

Reinhart RM, Carlisle NB, Kang MS, Woodman GF. Event-related potentials elicited by errors during the stop-signal task. II: Human effector specific error responses. *J Neurophysiol* 107: 2794–2807, 2012a.

Reinhart RM, Heitz RP, Purcell BA, Weigand PK, Schall JD, Woodman GF. Homologous mechanisms of visuospatial working memory maintenance in macaque and human: properties and sources. *J Neurosci* 32: 7711–7722, 2012b.

Sato T, Murthy A, Thompson KG, Schall JD. Search efficiency but not response interference affects visual selection in frontal eye field. *Neuron* 30: 583–591, 2001.

Sato TR, Schall JD. Effects of stimulus-response compatibility on neural selection in frontal eye field. *Neuron* 38: 637–648, 2003.

Schmolesky MT, Wang Y, Hanes DP, Thompson KG, Leutgeb S, Schall JD, Leventhal AG. Signal timing across the macaque visual system. *J Neurophysiol* 79: 3272–3278, 1998.

Theeuwes J. Top-down and bottom-up control of visual selection: reply to commentaries. *Acta Psychol (Amst)* 135: 133–139, 2010.

Thomas NWD, Pare M. Temporal processing of saccade targets in parietal cortex area LIP during visual search. *J Neurophysiol* 97: 942–947, 2007.

Thompson KG, Bichot NP. A visual salience map in the primate frontal eye field. *Prog Brain Res* 147: 249–262, 2005.

Thompson KG, Bichot NP, Schall JD. Dissociation of visual discrimination from saccade programming in macaque frontal eye field. *J Neurophysiol* 77: 1046–1050, 1997.

Thompson KG, Biscoe KL, Sato TR. Neuronal basis of covert spatial attention in the frontal eye field. *J Neurosci* 25: 9479–9487, 2005.

Thompson KG, Hanes DP, Bichot NP, Schall JD. Perceptual and motor processing stages identified in the activity of macaque frontal eye field neurons during visual search. *J Neurophysiol* 76: 4040–4055, 1996.

Treisman A, Gormican S. Feature analysis in early vision: evidence from search asymmetries. *Psychol Rev* 95: 15–48, 1988.

Treisman A, Sato S. Conjunction search revisited. *J Exp Psychol Hum Percept Perform* 16: 459–478, 1990.

Treisman AM, Gelade G. A feature-integration theory of attention. *Cogn Psychol* 12: 97–136, 1980.

Wardak C, Ibos G, Duhamel JR, Olivier E. Contribution of the monkey frontal eye field to covert visual attention. *J Neurosci* 26: 4228–4235, 2006.

Wardak C, Vanduffel W, Orban GA. Searching for a salient target involves frontal regions. *Cereb Cortex* 20: 2464–2477, 2010.

Wolfe JM. Guided search 4.0: current progress with a model of visual search. In: *Integrated Models of Cognitive Systems* , edited by Gray W. New York: Oxford, 2007, p. 99–119.

Wolfe JM. What can 1 million trials tell us about visual search? *Psychol Sci* 9: 33–39, 1998.

Woodman GF. Homologues of human ERP components in nonhuman primates. *The Oxford Handbook of ERP Components* . New York: Oxford University Press, 2011.

Woodman GF, Kang MS, Rossi AF, Schall JD. Nonhuman primate event-related potentials indexing covert shifts of attention. *Proc Natl Acad Sci USA* 104: 15111–15116, 2007.

Woodman GF, Kang MS, Thompson K, Schall JD. The effect of visual search efficiency on response preparation. *Psychol Sci* 19: 128–136, 2008.

Woodman GF, Luck SJ. Electrophysiological measurement of rapid shifts of attention during visual search. *Nature* 400: 867–869, 1999.

Woodman GF, Luck SJ. Serial deployment of attention during visual search. *J Exp Psychol Hum Percept Perform* 29: 121–138, 2003.

Young MH, Heitz R, Purcell B, Schall J, Woodman G. Source localization of an event-related potential indexing covert shifts of attention in macaques. *J Vis* 11: 194, 2011.

Zeki SM. Cortical projections from two prestriate areas in the monkey. *Brain Res* 34: 19–35, 1971.

Zhou H, Desimone R. Feature-based attention in the frontal eye field and area V4 during visual search. *Neuron* 70: 1205–1217, 2011.